Thermochimica Acta 479 (2008) 45–52

Contents lists available at ScienceDirect

Thermochimica Acta

journal homepage: www.elsevier.com/locate/tca

Non-isothermal crystallization kinetics and activity of filler in polypropylene/Mg–Al layered double hydroxide nanocomposites

M. Ardanuy*, J.I. Velasco, V. Realinho, D. Arencón, A.B. Martínez

Centre Català del Plàstic, Universitat Politècnica de Catalunya, C/Colom 114, E-08222 Terrassa, Spain

ARTICLE INFO

Article history:
Received 11 July 2008
Received in revised form
22 September 2008
Accepted 23 September 2008
Available online 30 September 2008

Keywords:
Layered double hydroxide
Polypropylene
Nanocomposites
Non-isothermal crystallization
Nucleation activity

ABSTRACT

The non-isothermal crystallization behaviour of Mg–Al layered double hydroxide (LDH)/polypropylene (PP) nanocomposites prepared by melt-dispersion was investigated through differential scanning calorimetry and discussed in comparison with that of montmorillonite (MMT)/PP ones. Combined effects of the LDH interlamellar modification and blending the PP with maleic anhydride-grafted PP (PP-g-MAH) and maleic anhydride-grafted poly(styrene-co-ethylenebutylene-co-styrene) (SEBS-g-MAH) were analysed. Different approaches were applied to determinate the crystallization kinetic parameters. The nucleation activity parameter indicated that LDH particle resulted active for heterogeneous nucleation of PP. Overall; the crystallization rate constant of the PP increased in presence of LDH in a similar extension that in presence of MMT nanoparticles. By applying an isoconversional method to the calorimetric data it was found that the effective activation energy decreased because of the effect of the nanoparticles and its value displayed different growing trends with the crystallization degree depending of the nanocomposite composition.

1. Introduction

Polypropylene (PP) is widely used in industry due to its well-balanced physical and mechanical properties, as well as to easy processing at a relatively low cost. The application of PP, however, has been limited by its high flammability, tendency to brittleness at temperatures below its glass transition temperature and low stiffness particularly at elevated temperatures. Traditionally, compounding PP with different inorganic particles has been of wide interest and it has been an effective way to improve thermal and mechanical properties of this polymer.

Nanocomposites consisting of PP matrix and natural or synthetic layered minerals like clays have been attracted much interest of researchers on the last decade. Mostly focused on cationic clays [1,2], and particularly on smectite-type layered silicates, clay-based fillers have recently been extended to the family of layered double hydroxides (LDH) [3] and different approaches to prepare LDH nanocomposites have been described in previous papers [4–10]. LDHs are a family of lamellar compounds containing exchangeable anions in the interlayer space (anionic clays). The structure consists of brucite-like sheets of typical thickness 0.5 nm, in which partial substitution of trivalent for divalent metallic ions results in a positive charge compensated by anions within interlayer galleries. The general formula is: $[M_{1-x}^{2+}\ M_x^{3+}(OH)_2][A_{x/n}^{n-}\cdot mH_2O]$, where M^{2+} and M^{3+} are di- and trivalent metal cations, respectively, that occupy octahedral positions in the hydroxide layers, and A^{n-} is an interlayer anion [11]. The nature of the layer metal ions can be changed among a wide possible selection and the interlayer anion can be also chosen among inorganic or organic species.

The melt-mixing preparation procedure of polymer/LDH nanocomposites include the LDH particle organophillization, consisting in swelling via ion exchange process with an anionic surfactant, followed by dispersion into a polymer matrix by applying high local shear stresses in a melt-mixer dispositive. These organophillized particles display an expanded crystalline structure because of the higher free volume of the interlamellar organic ion [8–10].

Owing to the low polarity of PP, it is usually necessary to use polar compatibilizer agents to promote strong interactions between the polymer melt and the particles, which ideally cause effective platelet dispersion within the melt matrix by shear and/or elongational mixing forces. Graft copolymers combining an identically or miscible part with functional groups capable to interact with the inorganic particle surface are usually used as compatibilizer [12–14].

Different studies have been focused on the effect of montmorillonite (MMT) and other smectite clays on the crystallization behaviour of PP nanocomposites. Most of them reported like silicate layers are active substrates for the heterogeneous nucleation of PP and PP-g-MAH. As a consequence, the polymer crystallization

* Corresponding author. Tel.: +34 937398158; fax: +34 937398101.
E-mail address: monica.ardanuy@upc.edu (M. Ardanuy).

0040-6031/$ – see front matter © 2008 Elsevier B.V. All rights reserved.
doi:10.1016/j.tca.2008.09.016

rate increases and the degree of surpercooling required for crystallizing decreases [10,15–18]. Differences in the Ozawa's exponent between PP and PP/clay nanocomposites indicated different mechanisms of crystal growth caused by the clay layer presence. The PP crystallization activation energy is usually found to decrease due to organophillized clay.

As far as we know, no studies about the effects of Mg–Al LDH nanoparticles on the crystallization behaviour of PP have been published. In the present paper, different PP/Mg–Al LDH and PP/MMT nanocomposites were prepared via melt mixing, and comparatively investigated their non-isothermal crystallization behaviour. The influence of different polymeric compatibilizers was also analysed. The nucleation activity of the particles, as well as the non-isothermal crystallization kinetic parameters, were determined and discussed. In addition, the activation energy was analysed through a differential isoconversional method.

2. Experimental

2.1. Materials

Isotactic poly(propylene) *Isplen PP 050* (MFI = 5.7 g/10 min) provided by Repsol-YPF (Puertollano, Spain) was used as a polymer matrix.

Three different polymer modifiers were used: maleic anhydride-grafted polypropylene (PP-g-MAH) (Epolene G-3003) supplied by Eastman Chemical; maleic anhydride grafted-poly[styrene-*b*-(ethylene-co-butylene)-*b*-styrene] triblock copolymer SEBS-g-MAH supplied by AKelastomer (Tuftec M1913) and poly(ethylene terephthalate-co-isophthalate) (PET) manufactured by Catalana de Polímers SL (El Prat de Llobregat, Spain).

Synthetic hydrotalcite supplied by Ciba (Hycite 713) with formula $[Mg_{0.7}Al_{0.3}(OH)_2](CO_3)_{0.15}{\cdot}nH_2O$ was used as Mg–Al LDH precursor.

2.2. Hydrotalcite and montmorillnonite organophillization

Organophillized hydrotalcite (HTDS) was prepared in two steps, combining the *reconstruction* method and the *ion exchange* one [11,19]. Firstly, calcined HT was stirred with NaCl salt in an aqueous solution to form LDH with chloride anions (HTCl). In a second step, the HTCl paste was stirred in a sodium dodecylsulfate aqueous solution at 80 °C for 3 days, employing a dodecylsulfate concentration two times that of the theoretical ion exchange capacity of HTCl. A white precipitate (the organophilic LDH) was isolated by filtration, washed with deionized water, dried under vacuum at 65 °C for 24 h and stored in a dessicator.

A fine high-purity bentonite fraction, rich in calcium MMT, was obtained from bentonite (natural clay from Minas de Gador, Spain) and ion-exchanged with undecyl ammonium chloride (OMMT) according to a previously published procedure [20].

2.3. Nanocomposite preparation

PP nanocomposites were prepared by melt-dispersion. A co-rotating twin-screw extruder (Collin ZK-35) with $D = 25$ mm and $L/D = 36$ was used. Intensive dispersive mixing was assured by means of three kneading blocks inserted in the screw configuration. A barrel temperature profile was selected from 150 °C at the polymer feeding to 190 °C at the end. Layered particles were fed in the extruder thought a feeding port located at a distance of 12*D* from the polymer feeding. Vacuum devolatilization was applied at a distance of 24*D*. The screw speed was fixed at 60 rpm. Under these conditions, the melt temperature measured at the die was never higher than 200 °C. A circular cross-section die of 3 mm diameter was employed. The extrudate was cooled in a water bath and pelletised. The composition of the resultant nanocomposites is shown in Table 1.

2.4. Measurement procedure

Differential scanning calorimetry (DSC) technique was used to perform non-isothermal crystallization experiments on the PP nanocomposites. A PerkinElmer Pyris 7 calorimeter was used. Calibration of the instrument was done using standard samples of In and Pb. The sample mass was typically 10 mg. Once the sample thermal history was erased for 3 min at 200 °C, cooling cycles were conducted from 200 to 30 °C, applying different cooling rates ranging from 5 to 40 °C/min. All runs were carried out in a stream of dried nitrogen. After each cooling, a heating run between 30 and 200 °C was performed at 10 °C/min. The crystallinity was calculated according to the following equation:

$$X_m = \frac{\Delta H_m (m_c/m_p)}{\Delta H_0} 100 \quad (1)$$

where ΔH_m was the melting enthalpy measured in the heating or cooling experiments, ΔH_0 is the theoretical enthalpy of PP 100% crystalline ($\Delta H_0 = 207.1$ J/g [21]), m_c is the mass of the sample and m_p is the mass of PP in the sample.

Table 1
Sample nomenclature, chemical composition and crystallization and melting characteristics at 10 °C/min.

Sample	Composition (wt.%)	Crystallization			Melting		
		T_c (°C)	$T_k - T_c$ (°C)	Δw (°C)	X_c (%)	T_m (°C)	X_m (%)
PP	PP	113.2	6.3	5.0	55.9	164.7	55.3
PPHT	PP/HT (90/10)	115.8	6.7	5.0	56.1	164.0	55.8
PPHTDS	PP/HTDS (90/10)	118.6	3.9	3.1	59.0	163.7	58.5
PPMHTDS	PP/PP-g-MAH/HTDS (88/2/10)	126.7	5.3	4.3	60.3	165.3	64.2
PPMHTDSD	PP/PP-g-MAH/HTDS (94/1/5)	125.0	5.1	4.7	62.0	165.5	65.5
PPSHTDS	PP/SEBS-g-MAH/HTDS (88/2/10)	118.6	4.9	3.6	60.0	163.9	62.1
PPSHTDSD	PP/SEBS-g-MAH/HTDS (94/1/5)	119.1	4.4	4.5	61.2	164.6	62.5
PPMMT	PP/MMT (96/4)	118.2	3.5	3.1	54.6	163.1	59.8
PPOMMT	PP/OMMT (96/4)	119.8	3.5	3.1	56.8	164.7	56.5
BMMMT	PP/PP-g-MAH/MMT (94/2/4)	118.8	4.3	4.4	56.9	163.4	61.0
BMOMMT	PP/PP-g-MAH/OMMT (94/2/4)	118.9	2.9	3.3	58.9	162.9	57.2
BPMMT	PP/PET/MMT (91/5/4)	122.8	3.5	4.6	58.8	165.1	58.5
BPOMMT	PP/PET/OMMT (91/5/4)	125.5	3.0	2.8	57.7	164.4	61.3
BMPMMT	PP/PP-g-MAH/PET/MMT (89/2/5/4)	122.5	3.2	3.3	62.2	163.7	59.0
BMPOMMT	PP/PP-g-MAH/PET/OMMT (89/2/5/4)	125.1	3.0	2.5	63.4	163.7	59.3

Also, the following parameters were measured: $T_k - T_c$ and Δw, T_c being the crystallization peak temperature and T_k the intercept of the base line with the tangent of the exotherm. This value gives information about the overall crystallization rate. Δw is the width at half height of the exotherm peak. As a general rule, a lower value of $T_k - T_c$ means faster overall crystallization rate, whereas a greater Δw value implies a broader crystalline size distribution.

3. Theoretical background

The Dobreva and Gutzow's nucleation activity parameter of the filler is defined as [22]:

$$\phi = \frac{B^*}{B^0} \tag{2}$$

The parameter B can be experimentally obtained from crystallization experiences through the following relationship proposed by Dobreva and Gutzow:

$$\log\ q = \text{const} - \frac{B}{2.3\Delta T^2} \tag{3}$$

where q is the crystallization rate, ΔT is the undercooling ($T_m - T_c$) with T_m the polymer melting temperature and T_c the crystallization peak temperature. In Eq. (2) B^* represent the value of B when the polymer crystallizes in presence of a nucleation substrate, and B^0 when there is no nucleation agent. The value of ϕ can vary from 1 to 0. It decreases as the nucleation activity increases. The approach was successfully applied to evaluate nucleating rate differences of PP containing different mineral fillers [20,23–27].

From the definition of B, the polymer crystal surface energy (σ) can be estimated:

$$B = \frac{16\pi\sigma^3 V_m^2}{3kT_m\Delta S_m^2 n} \tag{4}$$

and the lamella thickness (L), from the variant of the Gibbs–Thomson equation for a crystal of large lateral dimensions and finite thickness:

$$T_m = T_m^0\left[1 - \frac{2\sigma_e}{L\Delta H_m}\right] \tag{5}$$

In the above equations, k is the Boltzman's constant, T_m the PP melting temperature, ΔH_m the PP melting enthalpy and σ_e the specific surface energy. The PP molar volume (V_m) can be taken equal to 28 $cm^3\ mol^{-1}$, the molar entropy (ΔS_m) 24.2 $J\,K^{-1}$, the Avrami exponent $n = 3$, and the melting temperature at equilibrium (T_m^0) 479 K [25].

The Avrami equation was extended by Ozawa [28] to develop a simple method to characterize the non-isothermal crystallization kinetics assuming that the crystallization process is the result of an infinite number of isothermal crystallization steps. The degree of conversion at temperature T, $X(T)$, can be calculated as

$$1 - X(T) = \exp\left[\frac{-K(T)}{q^m}\right] \tag{6}$$

where the rate constant $K(T)$ is a function of the overall crystallization rate and m (Ozawa exponent) depends on the crystal growth dimensionality.

Plots of $\log[-\ln(1 - X(T))]$ versus $\log q$ at a given temperature should ideally result in straight lines, from which $K(T)$ and m parameters are obtained.

Ziabicki proposed a different variation of the Avrami's equation [29]:

$$\ln[-\ln(1 - X_t)] = \ln\ Z_t + n\ln t \tag{7}$$

where Z_t is a function related to the overall crystallization rate. Considering the non-isothermal character of the crystallization, the final form of the parameter characterizing the kinetics was given by Jeziorny [30]:

$$\ln\ Z_c = \ln\frac{Z_t}{q} \tag{8}$$

Liu and Juang [31] proposed a different theoretical kinetic model based on the combination of Ziabicki's and Ozawa's approaches:

$$\ln\ Z_t + n\ln t = \ln K(T) - m\ln q \tag{9}$$

$$\ln q = \frac{1}{m}\ln\left[\frac{K(T)}{Z_t}\right] - \frac{n}{m}\ln t \tag{10}$$

$$\ln q = \ln F(T) - b\ln t \tag{11}$$

where $F(T) = [K(T)/Z_t]^{1/n}$ refers to the crystallization kinetic parameter and b is the ratio of the exponents. Thus, a lower value of $F(T)$ means a higher crystallization rate.

Despite Kissinger's method has been widely applied in evaluating the activation energy of the crystallization processes, Vyazovkin has recently demonstrated its inapplicability on the processes that occur on cooling [32]. In this sense, reliable values of the effective activation energy can be obtained by using the isoconversional methods developed by Vyazovkin [32–34] and by Friedman [35]. These methods have been demonstrated to be appropriate to characterize the effective activation energy (E_α) on processes that occur on cooling.

In this paper, the Friedman method was used, due mainly to the simplicity of the method. This method has been used successfully in obtaining results on the effective energy barrier of PP/surface-treated SiO_2 nanocomposites [27] and aromatic polyesters [36].

The Friedman equation is expressed as

$$\ln\left(\frac{dX}{dt}\right)_X = \text{constant} - \frac{\Delta E_X}{RT_X} \tag{12}$$

where dX/dt is the instantaneous crystallization rate as a function of time at a given conversion X. According to this method, the $X(t)$ function obtained from the integration of the experimentally measured crystallization rates is initially differentiated with respect to time to obtain the instantaneous crystallization rate, dX/dt. Furthermore, by selecting appropriate degrees of crystallinity (i.e. from 1 to 95%) the values of dX/dt at a specific X are correlated to the corresponding crystallization temperature at this X, i.e. T_X. Then, by plotting the left hand side of Eq. (12) with respect to $1/T_X$ a straight line must be obtained with a slope equal to E_X/R.

Depending on the cooling rate, the same value of the relative degree of crystallinity (α) is accomplished at different temperatures. According to Vyazovkin and Sbirrazzuoli [34], T versus α dependence can be obtained by using an average temperature associated of the same value of relative degree of crystallinity (α). This dependence allows correlate the E_α with temperature. These plots can be used in evaluating Hoffman-Lauritzen parameters (K_g and U^*). The temperature dependence of the effective activation energy is defined as

$$E_\alpha(T) = U^*\frac{T^2}{(T - T_\infty)^2} + K_g R\frac{T_m^2 - T^2 - T_m T}{(T_m - T)^2 T} \tag{13}$$

where U^* is the activation energy of the segmental jump, T_∞ is a hypothetical at which viscous flow ceases (usually taken 30 K below the glass transition temperature, T_g), T_m is the equilibrium melting temperature and K_g is a kinetic parameter. This method was successfully used by Achilias et al. [37] to estimate the Hoffman–Lauritzen parameters from the overall rates of the non-isothermal crystallization of poly(propylene terepthalate) (PPT) and poly(butylene 2,6-naphthalate) (PBN).

Recently, Vyazovkin and Dranca [38] applied this method to non-isothermal data on both melt and glass crystallization and

these authors recommend the use of the melt and glass crystallization data as way of improving the precision and accuracy of the aforementioned approach to estimating the Hoffman–Lauritzen parameters. Nevertheless, taking into account that the main objective of this paper is to elucidate the effects of the LDH nanoparticles on the non-isothermal crystallization kinetics of PP, we have considered enough to compare the resulting parameters obtained for the melt crystallization data.

4. Results and discussion

4.1. Nucleation activity

In general, the presence of LDH and MMT particles resulted in higher crystallization peak temperature (T_c) of PP when cooled from the melt (Fig. 1), indicating some nucleation activity. Concerning PP/LDH nanocomposites, as can be seen in the values compiled in Table 1, the effect is more noticeable for the composites containing the organophillized Mg–Al LDH (HTDS) than the pure one (HT), indicating a more favourable crystal structure in HTDS than in HT to nucleate the PP crystallinity. The value of the lattice parameter *c* (corresponding to three times the spacing *d* between two consecutive layers of the LDH) determined by X-ray scattering, passed from 22.9 Å in HT to 84.6 Å in HTDS. This cell expansion of the nanoparticle could be the reason for a higher nucleation rate of the PP-α monoclinic crystal.

The effect of the polymer compatibilizer was found to be relevant. On one hand, the PP-g-MAH copolymer promoted an increase of 8 °C in the T_c values (samples PPMHTDS and PPMHTDSD), displaying the combination of HTDS particles with PP-g-MAH copolymer certain synergistic effect. In this sense, it has been reported that small amounts of PP-g-MAH could act as nucleating agents in PP [39]. On the other hand, SEBS-g-MAH did not display influence on the PP crystallization temperature (samples PPSHTDS and PPSHTDSD). The miscibility of PP-g-MAH in PP matrix could explain the greater influence excerted by this compatibilizer compared with SEBS-g-MAH one.

Concerning PP/MMT composites, different influences were observed depending on the composition. In the same way that LDH particles, MMT promoted the increasing of the PP crystallization peak temperature. The increase was slightly higher for the organophillized montmorillonite (OMMT). Contrarily to that found in PP/LDH nanocomposites, no effect of PP-g-MAH compatibilizer on the T_c value of PP/MMT nanocomposites was observed. Nevertheless, PET compatibilizer increased T_c value dramatically, mainly in the samples containing organophillized clay (OMMT). Similar results have been reported in PP/PET composites with other fillers [26], revealing nucleation activity of PET for PP.

Differences in the shape of the non-isothermal crystallization DSC signal resulted depending on the nanocomposite composition. From them, information about differences in the overall crystallization rate and crystal size distribution of the nanocomposites was obtained (Table 1). While pure Mg–Al LDH particles did not change the PP overall crystallization rate nor the crystalline size distribution, the organophillized ones caused a remarkable increased in the overall crystallization rate as well as a narrower crystalline size distribution, as revealed from the lower $T_c - T_k$ and Δw values. In general, when the compatibilizers were in the formulation the former effect was less marked, revealing that both the LDH organophillization and the polarity of the PP matrix had opposite influence on the crystallization behaviour. Unlike in PP/LDH nanocomposites, in PP/MMT ones the influence of both the particle organophillization and the compatibilizer presence was evident in terms of increased overall crystallization rate and narrower crystalline size distribution.

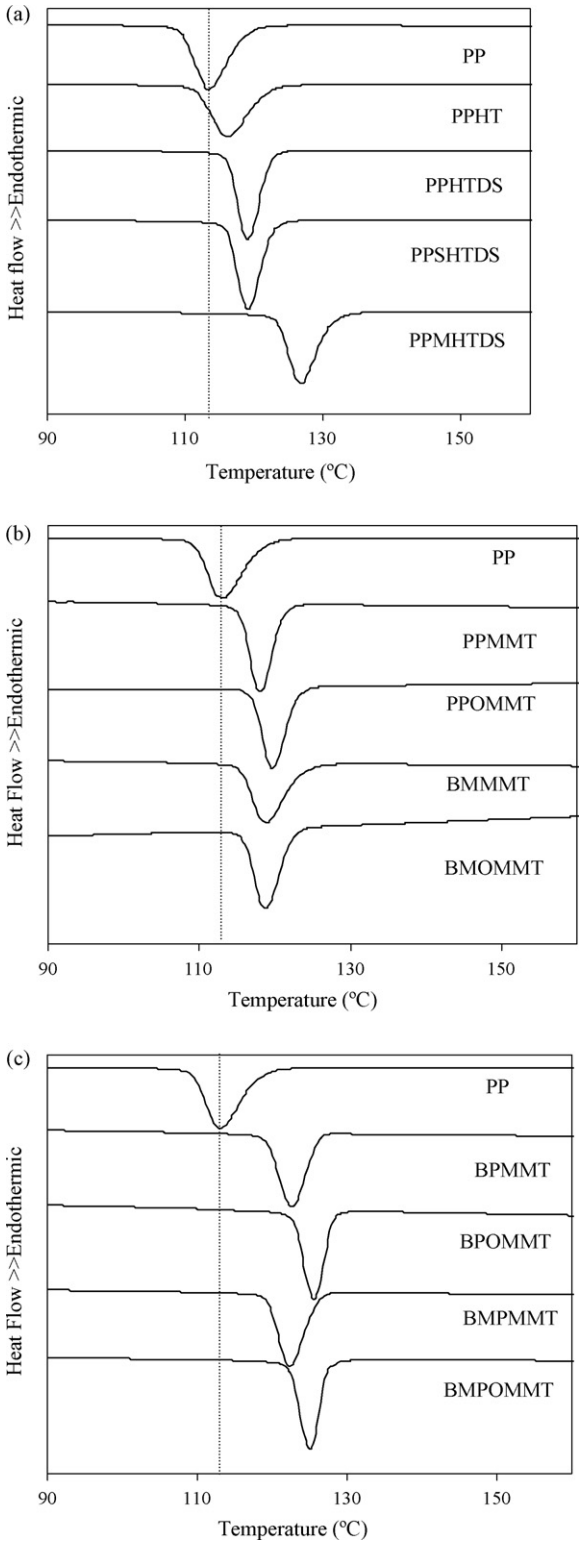

Fig. 1. DSC crystallization thermograms for (a) PP/LDH nanocomposites. (b) PP/MMT nanocomposites and (c) PP-PET/MMT nanocomposites, at cooling rate 10 °C/min.

The average crystalline fraction developed during non-isothermal crystallization of PP was slightly higher in the composites than in the pure polymer, which can be explained due to the effect of shifting the crystallization onset to higher temperatures (Table 1).

Table 2
Crystallization characteristics obtained by DSC.

Sample	Activity parameter, ϕ	Crystal surface energy, σ (10^{-6} J cm^{-2})	Lamellar thickness, L (10^{-9} m)
PP	1.00	2.11	4.71
PPHT	0.83	1.99	4.91
PPHTDS	0.87	2.01	4.43
PPMHTDS	0.47	1.67	4.06
PPMHTDSD	0.57	1.78	4.14
PPSHTDS	0.82	1.98	4.72
PPSHTDSD	0.82	1.97	4.38
PPMMT	0.92	2.05	4.35
PPOMMT	0.70	1.88	4.44
BMMMT	0.69	1.89	3.96
BMOMMT	0.78	1.97	4.53
BPMMT	0.75	1.93	4.57
BPOMMT	0.69	1.87	3.75
BMPMMT	0.76	1.96	4.46
BMPOMMT	0.69	1.90	4.53

As expected from the nucleation activity of both kinds of nanoparticles, values of ϕ-parameter resulted lower in the nanocomposites than in pure PP (Table 2). Similar results were obtained with surface-treated SiO_2 nanoparticles (ϕ 0.85) [27] or other particles like talc (ϕ 0.32) [23] or magnesium hydroxide (ϕ 0.52) [24].

For LDH nanocomposites, the values of activity parameter were similar for both untreated and organophillized LDH particle. The effect of the compatibilizer polymers on the ϕ-parameter was found to be different depending on the nature of the backbone. Whereas PP-g-MAH resulted in a dramatic lowering of ϕ value, SEBS-g-MAH showed no influence on this parameter. From these differences, one could accept that the high nucleation activity of PP-g-MAH should be due to its backbone molecular characteristics (i.e. low molecular weight) but not to interactions coming from the maleic anhydride group.

As a consequence of the differences in nucleation rate, both the calculated surface energy and the lamella thickness of PP crystal decreased in the nanocomposites (Table 2). Lower values of the nucleation activity parameter resulted in lower values of both crystal surface energy as well as lamella thickness.

Regarding MMT, the calculated ϕ values showed that the nucleation rate increased in this group of nanocomposites as follows: PP < PPMMT < BMOMMT < BMPMMT < PPOMMT < BMPOMMT. Therefore, the organophillization of the clay with undecyl ammonium affected the PP nucleation activity (PPMMT > PPOMMT and BMPMMT > BMPOMMT). As a consequence, both the surface energy and the calculated thickness value of PP crystal resulted lower in the nanocomposites prepared with organophillized MMT than in pure PP. When PET was used as a compatibilizer, the nucleation activity resulted improved, leading to a reduction of ϕ value. This effect was particularly remarkable in composites containing OMMT nanoparticles. However, combination of PET and PP-g-MAH did not result in further improvement. From these results, we can conclude that both LDH as MMT particle induce finer crystallinity in PP.

4.2. Analysis of crystallization kinetics

According to the analysis proposed by Ozawa, plots of $\log[-\ln(1-X(T)]$ versus $\log q$ resulted in straight lines with parallel relationship in the range between 116 and 122 °C (Fig. 2). From them, the kinetic parameters m and $K(T)$ were calculated (Table 3).

In general, the crystallization rate constant $K(T)$ of PP at a fixed temperature resulted increased with the presence of both LDH and MMT particles. The effect was found more noticeable

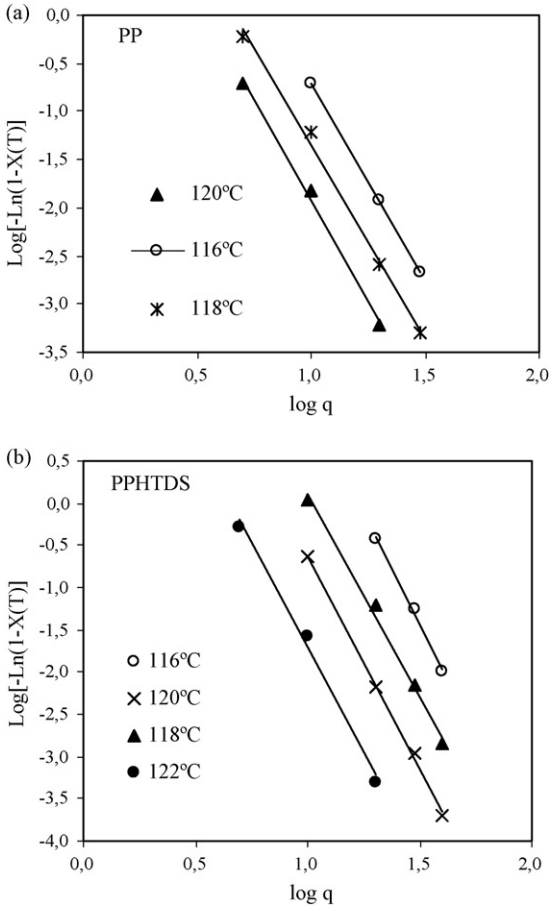

Fig. 2. Ozawa plos of $\log[-\ln(1-X(T)]$ versus $\log q$ for non-isothermal crystallization of (a) PP and (b) PPHTDS nanocomposite.

with the organophillized ones. The influence of the compatibilizer followed different trends. Whereas formulations containing PP-g-MAH displayed the lower $K(T)$ values, the PET containing MMT nanocomposites displayed the highest $K(T)$ values. Furthermore, no effect attributed to SEBS-g-MAH could be observed. These results seem to indicate that the studied nanoparticles, specially the organophillized ones, as well as the compatibilizers induce differences in the PP crystal growth rate.

The values of Ozawa exponent (m) for PP/LDH and PP/MMT nanocomposites at a fixed temperature were in general higher than the obtained for neat PP. Moreover, these differences increased in nanocomposites with presence of the organophillized particles. Therefore the type of nucleation and the growth mechanism of crystals in PP resulted strongly affected by the presence of these layered particles.

The kinetic parameters obtained from Ziabicki analysis are presented in Table 4. As could be expected, the value of Z_c increased with increasing cooling rates. Furthermore, for lower cooling rates (from 5 to 30 °C), Z_c resulted higher on nanocomposites compared with neat PP, confirming that, in general, the crystallization process of PP was accelerated because of the presence of LDH nanoparticles (Fig. 3).

Although the n exponent displayed a wide range of values, in general, at a fixed cooling rate, were higher for the nanocomposites, indicating differences on nuclei formation and spherulite grow of PP by the effects of the layered particles.

The $F(T)$ values obtained from Liu et al analysis (Table 4) systematically increased with the relative degree of crystallinity. Moreover, in general, at same relative degree of crystallinity, the values of $F(T)$

Table 3
Kinetic parameters of non-isothermal crystallization of PP/LDH and PP/MMT nanocomposites at different temperatures obtained from Ozawa analysis.

Sample	T (°C)	$K(T)$ (min^{-m})	m
PP	116	2,512	4.10
	118	457	4.01
	120	174	4.16
PPHT	116	1,514	3.63
	118	603	3.61
	120	309	3.80
PPHTDS	118	83,176	4.80
	120	23,988	5.01
	122	2,042	5.02
PPMHTDS	118	29,512	3.44
	120	5,754	3.28
	122	5,248	3.56
PPSHTDS	116	741,310	5.00
	118	77,625	5.00
	120	33,113	5.30
PPMHTDSD	116	9,121	2.42
	118	3,981	3.20
	120	1,230	3.30
PPSHTDSD	116	331,131	4.44
	118	44,668	4.33
	120	24,547	4.58
PPMMT	118	56,234	4.79
	120	4,266	4.72
	122	912	4.94
PPOMMT	118	3,235,937	5.64
	120	117,490	5.22
	122	10,233	5.16
BMMMT	118	6,310	3.64
	120	1,288	3.58
	122	933	3.91
BMOMMT	118	363,078	4.43
	120	11,482	4.84
	122	1,023	4.40
BPMMT	120	16,218	3.47
	122	3,236	3.47
	124	741	3.65
BPOMMT	122	20,417	3.33
	124	16,218	3.86
	126	2,188	3.99
BMPMMT	120	7,079	3.20
	122	2,570	3.39
	124	955	3.81
BMPOMMT	122	32,359	3.53
	124	28,840	4.23
	126	10,000	4.98

for LDH nanocomposites are lower than of neat PP, mainly for the samples with organophillized particles (Fig. 4). This means that to reach the same degree of crystallinity, $X(T)$, the crystallization time need by nanocomposites respect to neat PP is shorter, decreasing as follows: PP > PPHT > PPMHTDS ~ PPHTDS > PPSHTDS. These results are in agreement with the ones obtained from Ozawa and Ziabicki approaches analysed above, and indicate like both LDH and MMT particles, contribute to increase the overall crystallization rate of PP. Similar results were found in nanocomposites with MMT particles [15–18] or other nanoparticles [27].

4.3. Activation energy

The dependence of crystallization activation energy of PP on the extent of relative crystallization degree calculated using the Fried-

Table 4
Non-isothermal crystallization kinetic parameters obtained form Ziabicki and Liu et al. approaches for PP and PP/LDH nanocomposites.

Sample	Ziabicki			Liu et al.		
	q (°C/min)	n	Z_c (min^{-n})	X_t (%)	$F(T)$	B
PP	5	5.74	0.35	20	7.54	1.31
	10	5.81	0.83	40	9.58	1.29
	20	5.47	1.09	60	11.25	1.30
	30	5.08	1.12	80	13.20	1.33
	40	4.47	1.11			
PPHT	5	3.60	0.64	20	6.62	1.33
	10	3.55	1.01	40	8.67	1.29
	20	5.09	1.11	60	10.28	1.27
	30	4.62	1.14	80	12.06	1.27
	40	4.69	1.13			
PPHTDS	5	4.82	0.76	20	4.76	1.37
	10	4.70	1.16	40	5.93	1.37
	20	5.59	1.21	60	6.89	1.39
	30	5.19	1.18	80	8.17	1.43
	40	4.50	1.15			
PPMHTDS	5	2.89	0.81	20	4.39	1.06
	10	2.72	1.09	40	5.81	1.09
	20	2.54	1.12	60	7.03	1.13
	30	2.40	1.10	80	8.58	1.20
	40	2.31	1.06			
PPSHTDS	5	2.69	0.98	20	2.93	1.06
	10	2.40	1.14	40	3.99	1.18
	20	2.38	1.14	60	4.96	1.23
	30	2.24	1.11	80	6.11	1.30
	40	2.17	1.09			

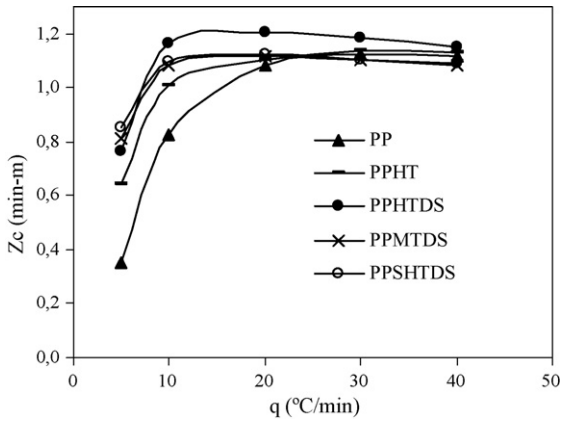

Fig. 3. Variation of the Z_c parameter calculated from Ziabicki analysis versus cooling rate for PP and PP/LDH nanocomposites.

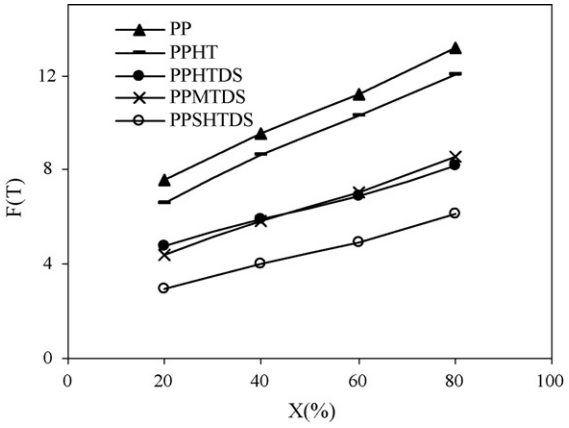

Fig. 4. Variation of the $F(T)$ parameter calculated from Liu et al. analysis versus the relative degree of crystallinity for PP and PP/LDH nanocomposites.

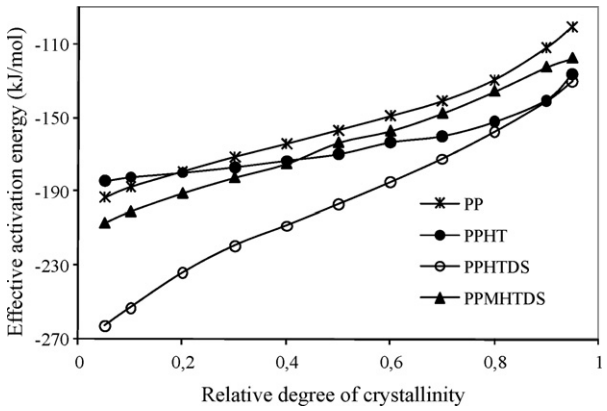

Fig. 5. Dependence of the effective activation energy on the relative extent of crystallization (isoconversional analysis) for PP and PP/Mg–Al LDH nanocomposites.

man's method is presented in Fig. 5. A growing trend of ΔE against the conversion degree can be observed for all studied samples. In addition, remarkable differences in the trends for the different nanocomposites resulted. In this sense, it is noticeable that in PPHTDS nanocomposite the ΔE value at the conversion onset is approximately 60 kJ mol^{-1} lower than that of the neat PP, but it reaches almost the same value at the end of the crystallization, indicating that the organophillized LDH particles are more effective in decreasing the activation energy at the early stages of the PP crystallization. By the other hand, pure LDH particles followed an opposite behaviour. From these results, it can be stated that the organophillized LDH particles induce easier crystallization in PP, either from the kinetics or from the energy point of view.

As aforementioned, an average temperature associated of the same value of relative degree of crystallinity (α) has been used to evaluate the T versus α dependence and to correlate the effective activation energy with temperature (Fig. 6). These plots have been used in evaluating the K_g and U^* parameters by Eq. (13) [34]. The graphics software Origin 7.0 has been employed to perform a non-linear curve fitting procedure. The theoretical lines fit the experimental data with the coefficient of determination (r^2) around 0.975. The fit yields the following parameters for pure PP: $K_g = 11.1 \times 10^5$ K^2, $U^* = 15.3$ kJ mol^{-1}. Meanwhile pure Mg–Al LDH particles contributed to decrease these values ($K_g = 7.2 \times 10^5$ K^2, $U^* = 2.3$ kJ mol^{-1} for PPHT) the organophillized ones acted in opposite way, being $K_g = 17.7 \times 10^5$ K^2, $U^* = 44.1$ kJ mol^{-1} for PPHTDS. The

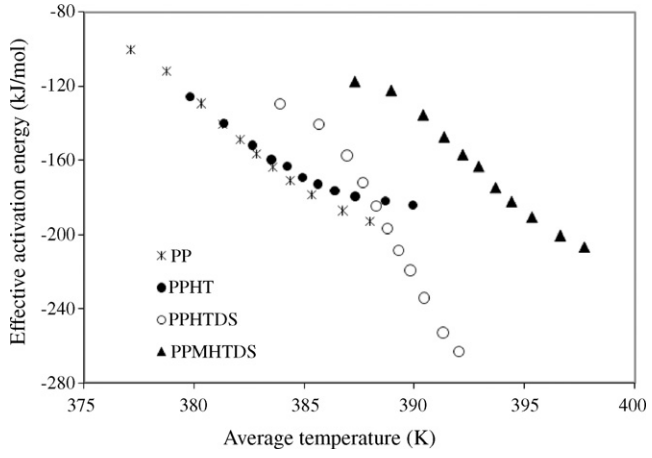

Fig. 6. Dependence of the effective activation energy on average temperature for PP and PP/Mg–Al LDH nanocomposites.

use of the combined PP-g-MAH and the organophillized Mg–Al LDH particles didn't cause significant changes on these parameters ($K_g = 10.5 \times 10^5$ K^2, $U^* = 16.4$ kJ mol^{-1} for PPMHTDS). These support the aforementioned effects of the organophillized Mg–Al LDH particles on the non-isothermal crystallization kinetics of PP.

5. Conclusions

The non-isothermal crystallization behaviour of PP/LDH and PP/MMT nanocomposites was studied. The analysis of the nucleation activity indicated that both LDH and MMT particles are active substrates for the heterogeneous nucleation of PP. The copolymer PP-g-MAH contributed to increase the nucleation activity in PP/LDH nanocomposites but displayed no appreciable effect on PP/MMT ones.

Kinetics parameters obtained from Ozawa and the other non-isothermal crystallization approaches provided an adequate description of the non-isothermal crystallization behaviour of PP nanocomposites. After the Ozawa analysis, the crystallization rate constant $K(T)$ increased in PP with the presence of both kind of nanoparticles, mainly with the organophillized ones. Values of Z_c and $F(T)$ obtained from Ziabicki and Liu et. analysis, respectively, supported the Ozawa results.

The effective activation energy decreased because of the effect of the nanoparticles. In addition, its value displayed different growing trends with the crystallization degree depending of the nanocomposite composition. The organophillization of the LDH particles had remarkable influence, not only on the dependency of the PP effective activation energy with the relative extent of crystallization, but also on its kinetics parameters.

References

[1] T.J. Pinnavia, G.W. Beall, Polymer–Clay Nanocomposites, John Wiley & Sons Ltd., New York, 2000.
[2] S.R. Suprakas, M. Okamoto, Prog. Polym. Sci. 28 (2003) 1539–1641.
[3] F. Leroux, J.P. Besse, Chem. Mater. 13 (2001) 3507–3515.
[4] H.B. Hsueh, C.Y. Chen, Polymer 44 (2003) 1151–1161.
[5] W. Chen, L. Feng, Q. Baojun, Chem. Mater. 16 (2004) 368–370.
[6] G.A. Wang, C.C. Wang, C.Y. Chen, Polymer 46 (2005) 5065–5074.
[7] F. Leroux, L. Meddar, B. Mailhot, S. Morlat-Thérias, J.L. Gardette, Polymer 46 (2005) 3571–3578.
[8] F.R. Costa, M. Abdel-Goad, U. Wagenknecht, G. Heinrich, Polymer 46 (2005) 4447–4453.
[9] L.C. Du, B.J. Qu, J. Mater. Chem. 16 (2006) 1549–1554.
[10] P. Ding, B. Qu, Polym. Eng. Sci. 9 (2006) 1153–1159.
[11] V. Rives, Layered Double Hydroxides: Present and Future, Nova Science Publishers Inc., New York, 2001.
[12] N. Hasegawa, H. Okamoto, M. Kato, A. Usuki, J. Appl. Polym. Sci. 78 (2000) 1918–1922.
[13] W. Xu, G. Liang, W. Wang, S. Tang, P. He, W.P. Pan, J. Appl. Polym. Sci. 88 (2003) 3093–3099.
[14] W.S. Chow, Z.A. Mohd-Ishak, J. Karger-Kocsis, A.A. Apostolov, U.S. Ishiaku, Polymer 44 (2003) 7427–7440.
[15] J. Li, C. Zhou, W. Gang, Polym. Test. 22 (2003) 217–223.
[16] J.D. He, M.K. Cheung, M.S. Yang, Q. Zongneng, J. Appl. Polym. Sci. 89 (2003) 3404–3415.
[17] D. Kaempfer, R. Thomann, R. Mülhaupt, Polymer 43 (2002) 2909–2916.
[18] C. Ding, D. Jia, H. He, B. Guo, H. Hong, Polym. Test. 24 (2005) 94–100.
[19] S.P. Newman, W. Jones, New J. Chem. 22 (1998) 105–115.
[20] J.I. Velasco, M. Ardanuy, L. Miralles, S. Ortiz, M.L. Maspoch, M. Sánchez-Soto, O. Santana, Macromol. Symp. 221 (2005) 63–73.
[21] B. Wunderlich, Thermal Analysis, Academic Press, New York, 1990.
[22] A. Dobreva-Veleva, I. Gutzow, J. Non Cryst. Solids 162 (1993) 13–25.
[23] M. Alonso, J.I. Velasco, J.A. de Saja, Eur. Polym. J. 33 (1997) 255–262.
[24] J.I. Velasco, C. Morhain, A.B. Martínez, M.A. Rodríguez-Pérez, J.A. de Saja, Macromol. Mater. Eng. 286 (2001) 719–730.
[25] J.I. Velasco, J.A. de Saja, A.B. Martínez, J. Appl. Polym. Sci. 61 (1996) 125–132.
[26] D. Arencón, J.I. Velasco, M.A. Rodríguez-Pérez, J.A. de Saja, J. Appl. Polym. Sci. 94 (2004) 1841–1852.
[27] G.Z. Papageorgiu, D.S. Achilias, D.N. Bikiaris, G.P. Karayannidis, Thermochim. Acta 427 (2005) 117–128.
[28] T. Ozawa, Polymer 12 (1971) 150–158.
[29] A. Ziabicki, Appl. Polym. Symp. 6 (1967) 1.

[30] A. Jeziorny, Polymer 19 (1978) 1142–1144.
[31] J.J. Liu, T.Y. Juang, Polymer 45 (2004) 7885–7887.
[32] S. Vyazovkin, Macromol. Rapid Commun. 23 (2002) 771–775.
[33] S. Vyazovkin, N. Sbirrazzuoli, J. Phys. Chem. B 107 (2003) 882–888.
[34] S. Vyazovkin, N. Sbirrazzuoli, Macromol. Rapid Commun. 25 (2004) 733–738.
[35] H.J. Friedman, Polym. Sci. C (1964) 183–195.
[36] P. Supaphol, N. Dangseeyun, P. Srimoaon, M. Nithitanakul, Thermochim. Acta 406 (2003) 207–220.
[37] D.S. Achilias, G.Z. Papageorgiou, G.P. Karayannidis, Macromol. Chem. Phys. 206 (2005) 1511–1519.
[38] S. Vyazovkin, I. Dranca, Macromol. Chem. Phys. 207 (2006) 20–25.
[39] M.A. López Manchado, M. Arroyo, Polymer 40 (1999) 487–495.